Cellular Physiology and Biochemistry

Cell Physiol Biochem 2017;44:1093-1105
DOI: 10.1159/000485415
Published online: November 27, 2017
Accepted: October 13, 2017

Original Paper

LukS-PV-Regulated MicroRNA-125a-3p Promotes THP-1 Macrophages Differentiation and Apoptosis by Down-Regulating NF1 and Bcl-2

Xiao-Xi Sun[a] Shan-Shan Zhang[b] Chun-Yang Dai[a] Jing Peng[a] Qing Pan[c] Liang-Fei Xu[a] Xiao-Ling Ma[a]

[a]Department of Laboratory Medicine, Anhui Provincial Hospital, Anhui Medical University, Hefei, [b]Sun Yat-sen University Cancer Center, Guangzhou, [c]Clinical Laboratory Center, The First Affiliated Hospital of Anhui University of Traditional Chinese Medicine, Hefei, China

Key Words
MicroRNA • LukS-PV • THP-1 • Differentiation • Apoptosis

Abstract
Background/Aims: LukS-PV is a component of Panton-Valentine leukocidin (PVL). We have previously demonstrated that LukS-PV potently promoted differentiation and induced apoptosis in THP-1 cells. However, the precise mechanisms of these actions remain unknown. MicroRNAs (miRs) play important roles in cellular differentiation and apoptosis. This study aimed to investigate the role of miR-125a-3p in LukS-PV-regulated differentiation and apoptosis and its underlying mechanism in THP-1 cells. ***Methods:*** MicroRNA profiling analyses were conducted to determine differential miRNA expression levels in THP-1 cells treated with LukS-PV. Cell differentiation and apoptosis were measured in THP-1 cells by gain-of-function and loss-of-function experiments. Bioinformatics analysis and luciferase reporter assays were used to confirm the targets of miR-125a-3p. The effects of the miR-125a-3p targets on cellular differentiation were determined by knocking them down. ***Results:*** MiR-125a-3p was up-regulated after treating the human monocytic leukaemia cell line THP-1 with LukS-PV. In addition, miR-125a-3p positively regulated apoptosis and differentiation in THP-1 cells treated with LukS-PV. Concordantly, luciferase reporter assays confirmed that neurofibromatosis type 1 (NF1) and B-cell lymphoma 2 (Bcl-2) were direct target genes of miR-125a-3p. Moreover, NF1 knockdown in THP-1 cells significantly promoted differentiation *in vitro*. Finally, the extracellular signal-regulated kinase (ERK) pathway, a downstream target of NF1, was activated after NF1 knockdown. ***Conclusions:*** These findings confirm that miR-125a-3p is involved in LukS-PV-mediated cell differentiation and apoptosis in THP-1 cells.

Xiao-Ling Ma

Department of Laboratory Medicine, Anhui Provincial Hospital, Anhui Medical University, No. 17 Lujiang Rd., Hefei, (China)
Tel. + 86 551 62283973, Fax + 86 551 62283973, E-Mail xiaolingma@126.com

Introduction

LukS-PV is a component of Panton-Valentine leukocidin (PVL), which is secreted by *Staphylococcus aureus* and targets human polymorph nuclear neutrophils (PMNs) [1]. Our previous studies have demonstrated that a long exposure (48 h) to LukS-PV resulted in THP-1 monocyte differentiation, and a short exposure (24 h) to LukS-PV led to THP-1 cell apoptosis [2, 3]. These results identified that LukS-PV plays a crucial role in THP-1 cell differentiation and apoptosis. However, its precise molecular mechanism has not been determined.

MicroRNAs (miRs) are 19–25 nucleotide, double-stranded non-coding RNAs that regulate gene products at the post-transcriptional level [4]. Variant miR expression is frequently observed in many types of cells and plays an important role in cellular differentiation and apoptosis [5, 6]. The biological function of miRs in THP-1 biological development involves the regulation of differentiation and apoptosis; for example, miR-149-5p inhibition induces apoptosis in THP-1 cells by targeting FASLG [7], and miR-199a-5p inhibition significantly promoted THP-1 monocyte differentiation into macrophages by targeting the activin A type 1B receptor gene [8]. In our study, we examined the differential expression of miRs using a miRNA expression profile analysis of THP-1 cells stimulated with LukS-PV. We found that microRNA-125a-3p (miR-125a-3p) expression was significantly increased more than that of any other miR. MiR-125a-3p, an isoform derived from the 3′-arm of pre-miR-125a, has been reported to be involved in apoptosis in various cells, such as the lung cancer cell line H1299, the glioma cell line U251, and the acute myeloid leukaemia cell lines HL-60 and NB4 [9-11]. Moreover, miR-125a-3p also regulates cell differentiation [12]. However, the role of miR-125a-3p in THP-1 cells treated with LukS-PV remains unknown.

THP-1, a human monocytic leukaemia cell line, best resembles primary monocytes. In addition, THP-1 cells are the most commonly utilized cell line to study monocyte/macrophage differentiation and function [13]. THP-1 cells have some major advantages over primary monocytes in experiments; these advantages include a homogenous genetic background that prevents donor variability and ensures reproducibility [14]. Monocytes and monocyte-derived macrophages play an essential role during infection, and their functions seem to be key factors in many immune disorders. Until now, the data on monocyte/macrophage dysfunction have been limited to a few reports, and the exact mechanism underlying these processes has not been proposed. However, recent studies have shown that miRs may be involved in the regulation of macrophage function. For example, the early secreted antigenic target 6-kDa protein (ESAT-6) promotes apoptosis in macrophages via targeting the miRNA155-SOCS1 interaction [15], microRNA-155 enhances the atherosclerosis inflammatory response in macrophages by targeting SOCS1 [16], and miR-146a regulates inflammation in macrophages by targeting TRAF6 [17]. In this study, we used THP-1 cells to investigate the role of miR-125a-3p in monocyte function after exposure to LukS-PV. Specifically, we focused on the effects of miR-125a-3p on apoptosis and differentiation. We also examined how LukS-PV regulates THP-1 cell differentiation and apoptosis through miR-125a-3p.

Materials and Methods

Cell culture

The human monocytic leukaemia cell line THP-1 was obtained from the Shanghai Institute for Biological Sciences (Shanghai, PR China). Cells were cultured in RPMI-1640 (Gibco, Grand Island, NY, USA) supplemented with 10% foetal bovine serum (FBS, HyClone, Logan, UT) and 1% penicillin/streptomycin in a humidified 5% CO_2 incubator at 37°C. Cells were passaged two to three times per week to maintain logarithmic phase growth.

Recombinant LukS-PV production and purification

pET28a (Roche Diagnostics Corp, Basel, Switzerland) was used to produce recombinant hexa-His-tagged LukS-PV. The sequence was amplified from PVL-positive *S. aureus* isolates. PCR products were

digested with XhoI and BamHI (Promega, Madison, WI, USA) and ligated into the pET28a vector. Recombinant LukS-PV purification was described previously by Ma et al [18]..

MicroRNA profiling analysis

THP-1 cells treated with 1.0 μM LukS-PV for 48 h and control cells were collected for microRNA profiling analysis. Total RNA extracted from THP-1 cells was reverse transcribed using the miRCURY Locked Nucleic Acid (LNA™) Universal Reverse Transcription microRNA PCR, Polyadenylation and cDNA synthesis kit (Exiqon). Then, to identify differentially expressed miRNAs, the samples were subjected to the Exiqon miRCURY Ready-to-Use PCR Human Panel I+II (Exiqon miRNA qPCR panel, Vedbaek, Denmark), which could detect 772 miRNAs in cells, and run on a 7900HT real-time PCR system (Applied Biosystems, Foster City, CA, USA). The method used 384-well PCR plates, and pre-aliquoted LNA™ PCR primers were added to each well. cDNA was pre-amplified by SP6 primers. After identifying Ct reunification values, follow-up experiments were performed. The fold-change in the expression of each miRNA was calculated by using the $2^{-\Delta\Delta Ct}$ method. MiRs were considered to be up-regulated or down-regulated if the changes in expression were ≥ 2.0-fold or ≤ 2.0-fold, respectively.

RNA isolation and real-time RT-PCR

Total RNA was extracted using TRIzol (Invitrogen) according to the manufacturer's instructions. Reverse transcription for gene expression or miR expression was performed using the RevertAid First Strand cDNA Synthesis Kit (Fermentas, Vilnius, Lithuania). All RT-PCR reactions were carried out using a StepOnePlus RT-PCR system (Applied Biosystems, Carlsbad, CA, USA). To measure gene expression, quantitative real-time PCR (RT-qPCR) was conducted using the SYBR Green PCR Kit (QIAGEN, Hilden, Germany) according to the manufacturer's protocol. The data were processed by the comparative cycle threshold method and are expressed as fold increases relative to the basal transcription level. The amount of target mRNA was normalized to GAPDH. For quantitative RT-PCR of miRs, the cDNA products used for PCR were generated as described before. miR expression was measured using the TaqMan miRNA Kit (GenePharma, Shanghai, PR China) according to the manufacturer's instructions. Mature miRs were normalized to U6-snRNA. Relative expression was calculated using the comparative Ct method. All the primer sequences used in this study are listed in Table 1.

Lentiviral transduction

THP-1 cells were transduced with lentiviral vectors expressing *has*-miR-125a-3p, an inhibitor of *has*-miR-125a-3p expression or an neurofibromatosis type 1 (NF1)-targeting shRNA (Genechem, Shanghai, PR China). Lentiviruses at a multiplicity of infection (MOI) between 50 and 70 were added to THP-1 cells at 37°C. For controls, lentiviral vectors containing short hairpin sequences targeting a non-mammalian gene were used at similar MOIs. Cells were infected for 24 h and then maintained in culture medium.

Table 1. Primer sequences for PCR

Primers	Sequences 5' → 3'
Has-miR-125a-3p-F	ATCTGACACAGGTGAGGTTCTTG
Has-miR-125a-3p-R	TATGGTTTTGACGACTGTGTGAT
Has-miR-181a-3p-F	AGAATTACACCATCGACCGTTG
Has-miR-181a-3p-R	TATGCTTGTTCTCGTCTCTGGTC
Has-miR-761-F	ATTACTTGCAGCAGGGTGAAAC
Has-miR-761-R	TATGCTTGTTCTCGTCTCTGTGTC
U6-F	ATTGGAACGATACAGAGAAGATT
U6-R	GGAACGCTTCACGAATTTG
GAPDH-F	GGAGCGAGATCCCTCCAAAAT
GAPDH-R	GGCTGTTGTCATACTTCTCATGG
NF1-F	CACTGGTCCAGCCTTAACCT
NF1-R	TAGGATTCCCAGCTTTGGAG
Bcl-2-F	GAAGCACAGATGGTTGATGC
Bcl-2-R	CAGCCTCACAAGGTTCCAAT

Morphology assay

Cells were cultured at a density of 1 × 10^6 cells per well in six-well plates. Cell morphology was examined by staining with a modified Wright-Giemsa solution and using an optical microscope (Nikon, Tokyo, Japan).

Flow cytometry

For immunophenotyping, cells were harvested by centrifugation at 1000 × *g* for 5 min, washed twice in cold PBS,

resuspended in 200 µl of PBS and co-stained with CD11b-APC and CD14-PE (eBioscience, San Diego, CA, USA) at 4°C for 1 h in the dark. Cells were washed twice with cold PBS to prevent non-specific binding, and the stained samples were run on a FACS Calibur flow cytometer (BD Biosciences, San Jose, CA, USA) according to the manufacturer's instructions. The data were analysed using FlowJo Express software (FlowJo Inc., Ashland, OR, USA).

Western blotting

After the various treatments, cells were lysed in lysis buffer with protease inhibitor cocktail, 1 mmol/L sodium fluoride and 1 mmol/L sodium orthovanadate. Proteins (40 µg) were separated on 12% SDS-polyacrylamide gels and electrophoretically transferred onto polyvinylidene difluoride membranes (Millipore, Bedford, MA, USA). The membranes were blocked with 10% milk in Tris-buffered saline/0.1% Tween-20 for 2 h and subsequently probed with primary antibodies. Then, the membranes were incubated with a horseradish peroxidase-conjugated secondary antibody for 1 h. Immunoreactive bands were visualized with an enhanced chemiluminescence detection system. All of the rabbit anti-human primary antibodies were purchased from Cell Signaling Technology.

Cell cycle analysis

The cells were harvested by centrifugation at 2000 rpm for 10 min, washed twice with cold PBS, and resuspended in cold 75% ethanol. Cell cycle analyses were performed using the BD Pharmingen™ PI/RNase staining buffer and flow cytometry according to the manufacturer's instructions.

Caspase-3 activity assay

Caspase-3 activity was measured by fluorometric assay (Beyotime Biotechnology, Shanghai, PR China) according to the manufacturer's instructions. Briefly, cells were homogenized with lysis buffer, and lysates were centrifuged at 20000 × *g* for 15 min at 4°C. Subsequently, the supernatants were treated with Ac-DEVD-pNA at 37°C for 6–8 h. Samples were read at 405 nm (ELX808U, Bio-Tek, USA). Caspase activation is expressed as the relative increase compared with the controls.

MiR-125a-3p target prediction and luciferase reporter assays

Three bioinformatics databases were used for the *in silico* prediction of miR-125a-3p targets: miRBase, miRanda and TargetScan. Predicted target genes that were common in at least 2 of the 3 databases were chosen for luciferase assays. For the luciferase assays, HEK 293T cells were transfected with miR-125a-3p mimics or with the empty miR non-specific control (NC) (GenePharma) and wild-type, mutated NF1 or B-cell lymphoma 2 (Bcl-2) 3′-UTR plasmids (constructed by GenePharma) using Lipofectamine 2000 (Life Technologies, Carlsbad, CA, USA). Luciferase activities were measured at 24 h post-transfection using the dual-luciferase assay system (Promega, Madison, WI, USA). Luminescence readings were acquired using a Flexstation 3 Multiscan Spectrum (Molecular Devices, Sunnyvale, CA, USA).

Statistical analysis

All data are expressed as the mean ± standard deviation (SD), and all experiments were performed in triplicate. Statistical analyses shown in the figures were performed using t-tests or one-way ANOVA. All statistical analyses were conducted using SPSS 16.0 (SPSS Inc., Chicago, IL, USA). A value of $p < 0.05$ was considered statistically significant.

Results

Identification of differential miR-125a-3p expression in LukS-PV-treated THP-1 cells

We examined the expression levels of 772 miRs in LukS-PV-treated THP-1 cells *in vitro* through miRNA expression profile analysis. We found that 161 miRs were up-regulated, whereas 35 miRs were down-regulated. The scatterplot and cluster graph of the profile results are shown in Fig. 1A and 1B. The data showed that the miR with the highest-fold increase was miR-125a-3p (102.5-fold), followed by miR-181a-3p (58.79-fold); miR-761 showed the highest-fold decrease (18.82-fold). These findings indicated that these

differentially expressed miRs might be associated with THP-1 cell differentiation and apoptosis induced by LukS-PV. To validate the results of the miRNA expression profile, we measured the expression levels of miR-125a-3p, miR-181a-3p and miR-761 in THP-1 cells treated with 1.0 μM LukS-PV for 48 h by real-time RT-PCR. These results were inconsistent with the profile analysis regarding the specific fold changes because of the different methods and test frequency. However, as shown in Fig. 1C, the tendency of the miRs to increase or decrease was consistent with the profile analysis. For this study, we selected miR-125a-3p and investigated its role in the effects of LukS-PV on THP-1 cells.

MiR-125a-3p is involved in the differentiation of LukS-PV-treated THP-1 cells

To investigate whether miR-125a-3p expression is correlated with THP-1 cell differentiation, THP-1 cells were transfected with miR-125a-3p over-expression or miR-125a-3p NC lentiviral vectors. Wright-Giemsa staining was first used to evaluate the differentiation potential of the two cell populations. As shown in Fig. 2A, cells in the miR-125a-3p-over-expressing group exhibited greater cytoplasmic-to-nuclear ratios and larger sizes than cells in the miR-NC group, which appeared to be predominantly myelocytes with round, regular cell margins and large nuclei. Then, we calculated the percentages of differentiated cells

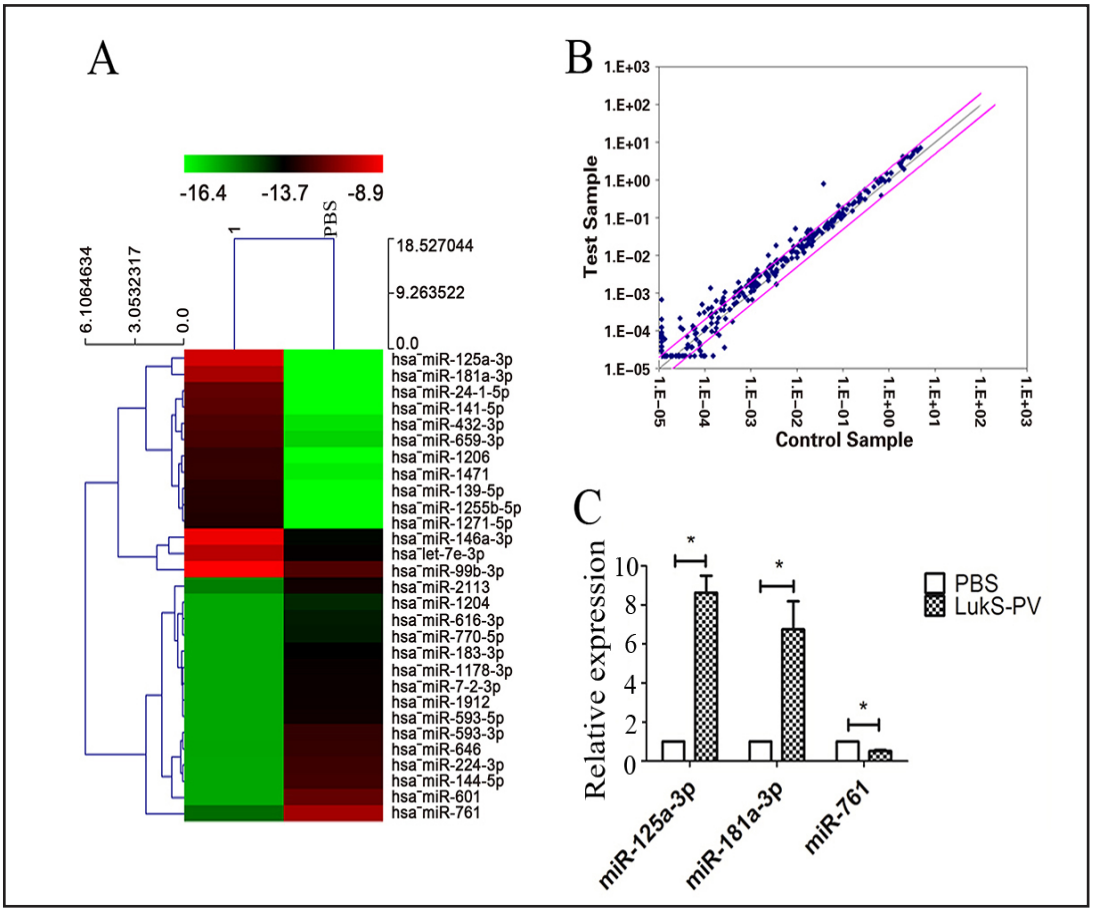

Fig. 1. MiRNA expression profile analysis in LukS-PV-treated THP-1 cells. Differences between groups were considered significant if a 2-fold variation was observed. (A) Heatmap representation of the 29 most differentially expressed miRNAs. (B) Scatter diagram representation of the differentially expressed miRNAs. Cut-off levels are shown with red lines. Specific miRNA expression levels were higher in the treatment group (black dots) than in the control group. (C) MiR-125a-3p, miR-181a-3p and miR-761 expression levels in THP-1 cells incubated with 1.0 μM LukS-PV for 48 h were assessed by RT-PCT to validate the results of the miRNA expression profile analysis. *p < 0.05.

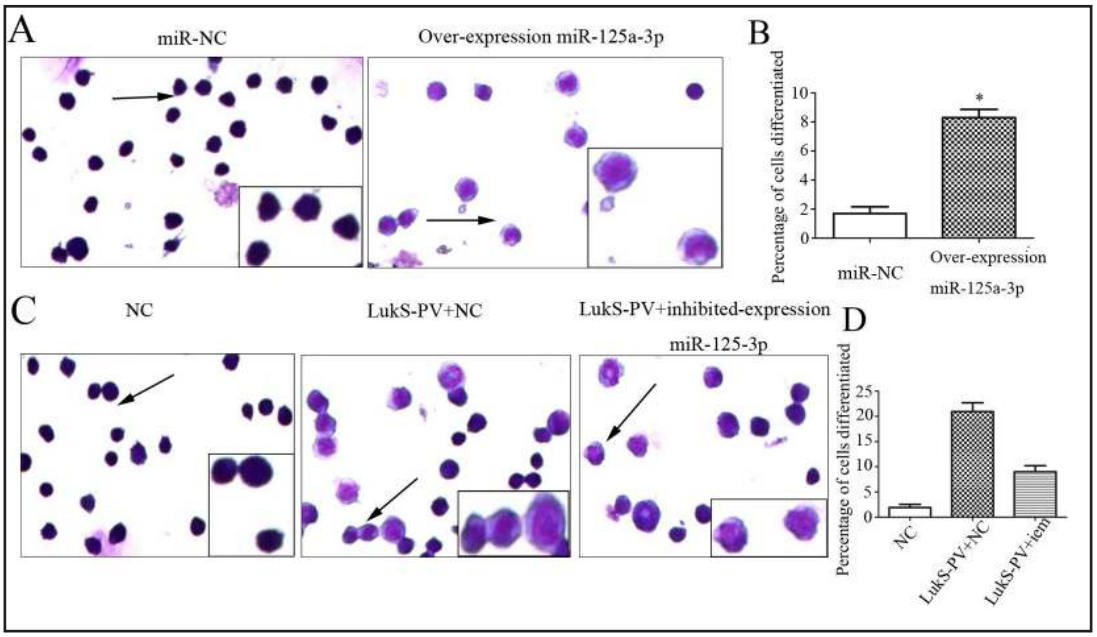

Fig. 2. LukS-PV-regulated microRNA-125a-3p regulates morphological changes in THP-1 cells. (A and C) Representative images show the characteristic morphology of differentiated cells. (B and D) Percentages of differentiated cells in (A and C) are expressed as the mean ± SD of three independent experiments. iem indicates the inhibition of miR-125a-3p expression.

in each group. The percentage of differentiated cells was increased to 8.36% in the miR-125a-3p-over-expressing group but to only 1.78% in the miR-NC group (Fig. 2B). Next, flow cytometry and western blotting assays were used to further investigate the differentiation potential of the two cell populations. As shown in Fig. 3A and 3C, miR-125a-3p over-expression clearly increased the expression levels of the cell surface differentiation antigens CD11b and CD14 and up-regulated the phosphorylation levels of the differentiation-related proteins extracellular signal-regulated kinase (ERK), c-JUN and c-FOS.

To validate whether the LukS-PV-mediated induction of THP-1 cell differentiation required miR-125a-3p activity, miR-125a-3p was silenced by transfecting an inhibitory miR-125a-3p construct. Then, the effects of LukS-PV on differentiation marker expression levels were determined as before. First, we carried out a morphology analysis. As shown in Fig. 2C, obvious differentiation was observed in the cells treated with 1.0 μM LukS-PV for 48 h. These cells had an increased cytoplasmic/nuclear ratio and chromatin condensation. Differentiation was significantly decreased in the cells expressing the miR-125a-3p-inhibiting construct and incubated with LukS-PV. Next, we calculated the percentages of differentiated cells in each group. The percentage of differentiated cells was increased from 2.38% to 21.38% after LukS-PV treatment but was then decreased to 8.78% when the miR-125a-3p-inhibiting construct was added (Fig. 2D). Additionally, in THP-1 cells treated with LukS-PV, silencing miR-125a-3p considerably suppressed CD11b and CD14 expression (Fig. 3D). Moreover, the levels of phosphorylated ERK, c-JUN and c-FOS (Fig. 3F) were also reduced. These results demonstrate that the up-regulation of miR-125a-3p may be responsible for the effects of LukS-PV on differentiation in THP-1 cells.

MiR-125a-3p is involved in cell cycle and apoptosis regulation in LukS-PV-treated THP-1 cells

Our previous study confirmed that LukS-PV could induce cell cycle arrest and apoptosis in THP-1 cells. To investigate whether miR-125a-3p is involved in these processes, we examined the cell cycle phase distribution of treated cells by flow cytometry. Caspase-3

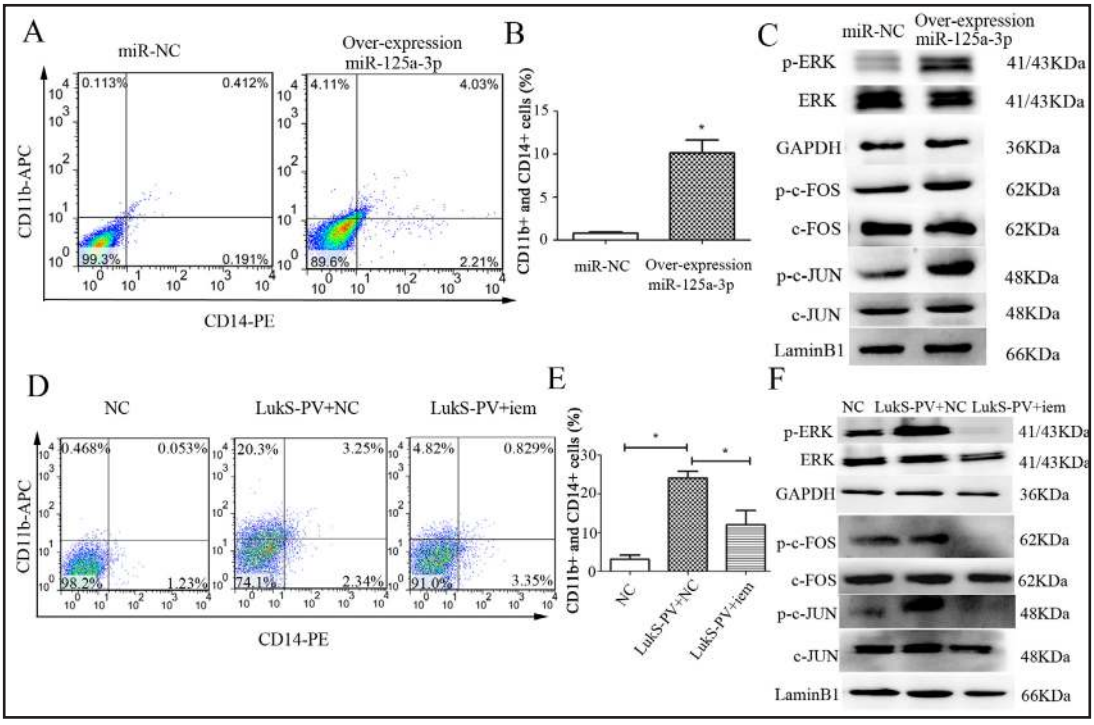

Fig. 3. LukS-PV-regulated microRNA-125a-3p promotes THP-1 cell differentiation by activating ERK signalling. (A) MiR-125a-3p over-expression increased CD11b and CD14 expression levels (C) and up-regulated ERK, c-JUN and c-FOS phosphorylation. (B) Percentages of $CD11b^+$ and $CD14^+$ cells in (A) are expressed as the mean ± SD of three independent experiments. (D) Silencing miR-125a-3p in THP-1 cells treated with 1.0 μM LukS-PV for 48 h largely inhibited CD11b and CD14 expression (F) and down-regulated ERK, c-JUN and c-FOS phosphorylation. (E) Percentages of $CD11b^+$ and $CD14^+$ cells in (D) are expressed as the mean ± SD of three independent experiments. *p<0.05. iem indicates the inhibition of miR-125a-3p expression.

activity and western blotting assays were used to measure the expression levels of apoptotic markers. The results showed that miR-125a-3p over-expression significantly induced G0/G1 phase arrest and decreased the percentage of cells in the S phase (Fig. 4A and 4B). Moreover, as shown in Fig. 5A and 5B, miR-125a-3p over-expression also significantly increased caspase-3 activity and expression levels of the pro-apoptotic proteins caspase-3, caspase-8, caspase-9 and Bax; miR-125a-3p over-expression decreased the expression levels of the anti-apoptotic protein Bcl-2 in THP-1 cells.

When blocking the function of miR-125a-3p by transfecting the targeted miR sponge into THP-1 cells, the effects of LukS-PV on cell cycle and apoptosis were remarkably reduced. As shown in Fig. 4C and 4D, after the miR-125a-3p-inhibited group was treated with LukS-PV for 24 h, the percentage of cells in the G0/G1 phase decreased but increased in the S phase. In addition, the caspase-3 activity and pro-apoptotic protein levels decreased, whereas the expression of anti-apoptotic proteins increased in the miR-125a-3p-inhibited group after LukS-PV treatment for 24 h (Fig. 5C and 5D). These findings strongly suggest that miR-125a-3p up-regulation may be involved in the LukS-PV-mediated cell cycle and apoptosis regulation in THP-1 cells.

MiR-125a-3p directly targets NF1 and Bcl-2

MiRs generally exert their function by blocking the expression of their target genes. To investigate the targets of miR-125a-3p in THP-1 cells, a bioinformatics prediction was used to analyse and identify potential target genes. From these results, we found that the NF1

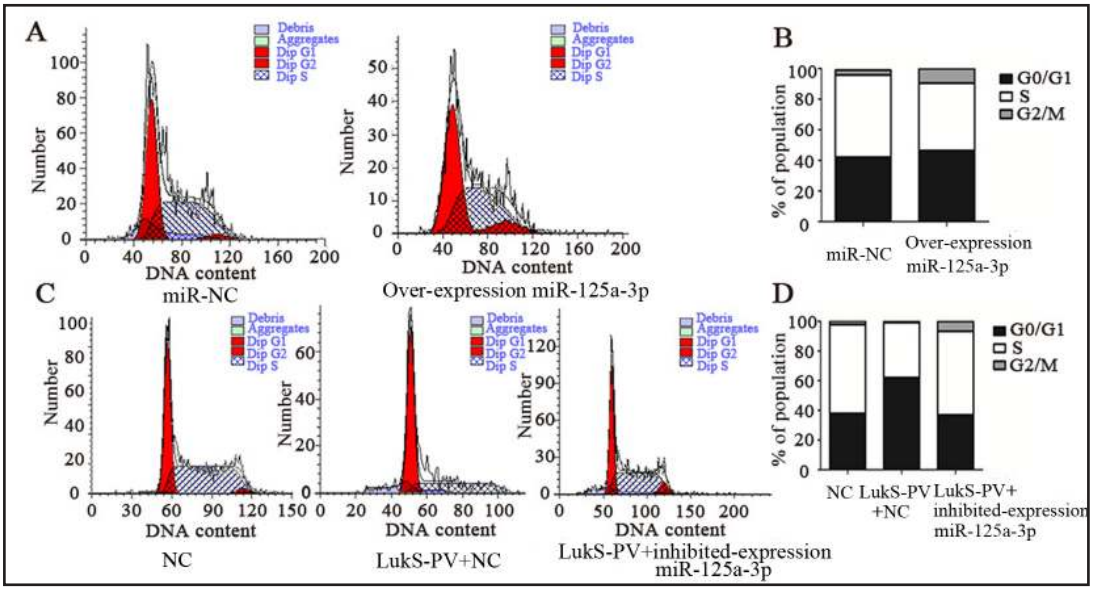

Fig. 4. MiR-125a-3p is involved in cell cycle regulation in LukS-PV-treated THP-1 cells. (A) miR-125a-3p over-expression induced G0/G1 phase arrest and a decrease in the percentage of cells in the S phase. (C) Silencing miR-125a-3p in THP-1 cells treated with 1.0 μM LukS-PV for 24 h promoted a decrease in the percentage of cells in the G0/G1 phase and an increase in the percentage of cells in the S phase. (B, D) Distribution of cells in the G0/G1 (black), S (white), and G2/M (grey) phases of cell cycle progression.

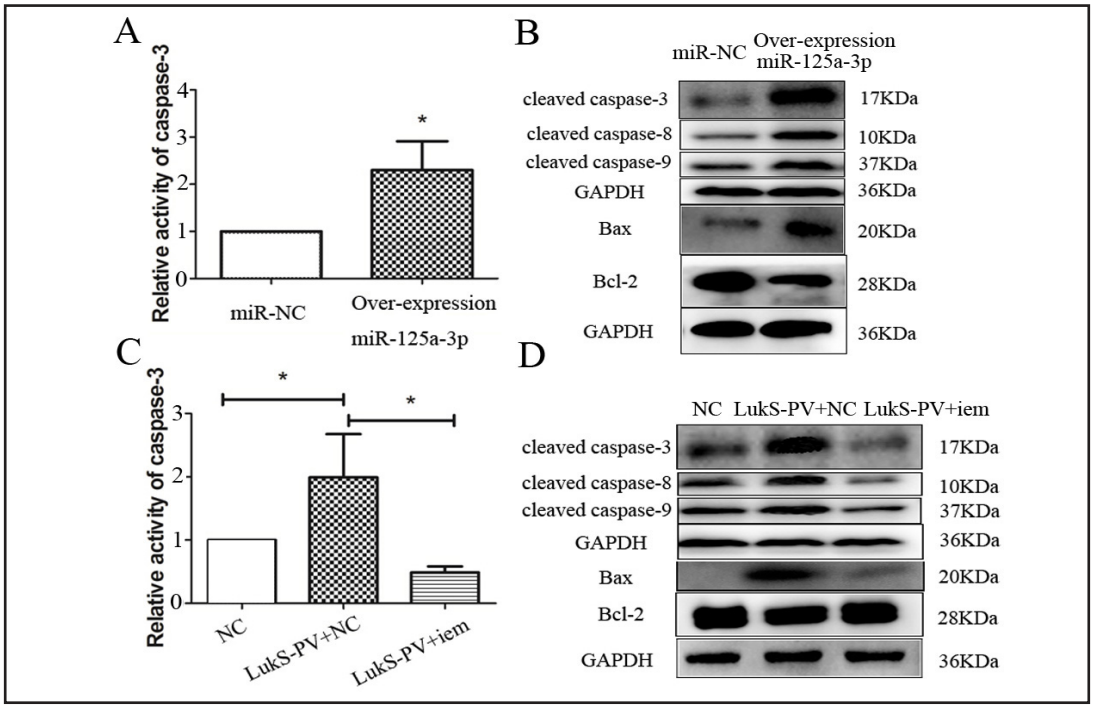

Fig. 5. LukS-PV-regulated microRNA-125a-3p promotes THP-1 cell apoptosis. (A) MiR-125a-3p over-expression increased caspase-3 activity in THP-1 cells, (B) increased the expression levels of the pro-apoptotic proteins caspase-3, caspase-8, caspase-9 and Bax and decreased the expression levels of the anti-apoptotic protein Bcl-2. (C) Silencing miR-125a-3p in THP-1 cells treated with 1.0 μM LukS-PV for 24 h considerably inhibited caspase-3 activity, (D) down-regulated caspase-3, caspase-8, caspase-9 and Bax expression and up-regulated Bcl-2 expression. The experiments were repeated three times. *p<0.05. iem indicates the inhibition of miR-125a-3p expression.

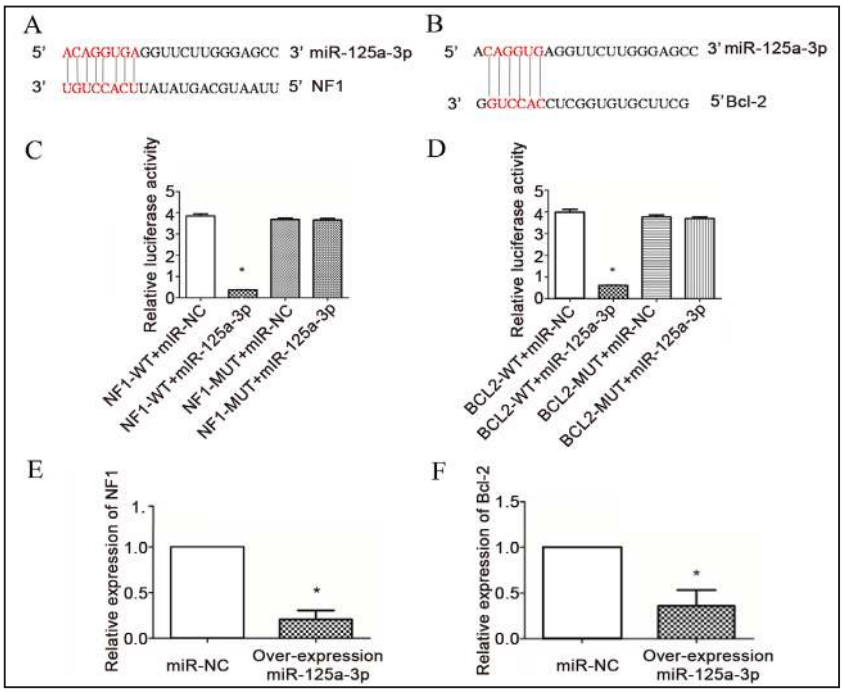

Fig. 6. NF1 and Bcl-2 are direct targets of miR-125a-3p. The highly conserved miR-125a-3p binding motif in the 3′-UTR of (A) NF1 and (B) Bcl-2, as predicted by bioinformatics databases. MiR-125a-3p suppressed the activity of firefly luciferase that carried the wild-type but not the mutant 3′-UTRs of NF1 (C) and Bcl-2 (D). RT-qPCR results showing a significant inverse correlation between miR-125a-3p and NF1 (E) and (F) Bcl-2 expression in THP-1 cells. The experiments were repeated three times. *p<0.05.

and Bcl-2 3′-untranslated regions (3′-UTRs) contained sites complementary to miR-125a-3p (Fig. 6A and 6B).

To validate whether NF1 and Bcl-2 are targets of miR-125a-3p, we separately cloned fragments of the NF1 and Bcl-2 3′-UTRs that contained wild-type or mutated miR-125a-3p-binding sequences into the psi-CHECK2 luciferase reporter plasmid. When the miR-125a-3p mimics were co-transfected with the reporter plasmid into HEK 293T cells, the relative luciferase activities of the reporter containing the wild-type NF1 or Bcl-2 3′-UTRs were significantly suppressed; however, the luciferase activities of the reporter containing the mutated NF1 or Bcl-2 3′-UTRs were unaltered (Fig. 6C and 6D). These findings indicate that miR-125a-3p directly targets the 3′-UTRs of NF1 and Bcl-2.

To further verify the relationship between miR-125a-3p and NF1 and Bcl-2, qRT-PCR was performed to examine the effects of miR-125a-3p over-expression on NF1 and Bcl-2 expression levels in THP-1 cells. The data showed a significant inverse correlation between miR-125a-3p expression and NF1 and Bcl-2 mRNA levels (Fig. 6E and 6F). These results demonstrate that miR-125a-3p can directly down-regulate NF1 and Bcl-2 expression in THP-1 cells.

NF1 loss promotes differentiation by activating the ERK pathway in THP-1 cells

NF1 is a GTPase activating protein that terminates Ras signalling. Few studies have investigated the role of NF1 in acute myelogenous leukaemia (AML) cell differentiation. To investigate the relationship between NF1 and THP-1 cell differentiation, we knocked down NF1 in THP-1 cells and conducted functional experiments. NF1 expression was decreased by 50% in THP-1 cells transfected with NF1 knockdown (KD) lentiviral vectors compared with that in cells transfected with the NC vectors (Fig. 7A). As shown in Fig. 7B and 7C, NF1 knockdown increased CD11b and CD14 expression levels and up-regulated the phosphorylation of the differentiation-related proteins ERK, c-JUN and c-FOS. These results suggested that down-regulating NF1 promoted THP-1 cell differentiation by activating the ERK pathway.

Discussion

PVL consists of two components, LukS-PV and LukF-PV. During infection, LukS-PV specifically binds to receptors on the plasma membrane of PMNs and then combines with LukF-PV to form an octamer that plays a key role in membrane perforation [19]. Recent studies have demonstrated that sublytic amounts of PVL can activate protective host immunity and enhance PMN phagocytosis [20, 21]. LukS-PV is not cytotoxic when used alone [1, 19, 22]. Our earlier work on LukS-PV was the first report to demonstrate that it promotes differentiation and apoptosis in THP-1 cells *in vitro* [2, 3]. However, the precise mechanisms through which LukS-PV exerts these functions in THP-1 cells are poorly understood.

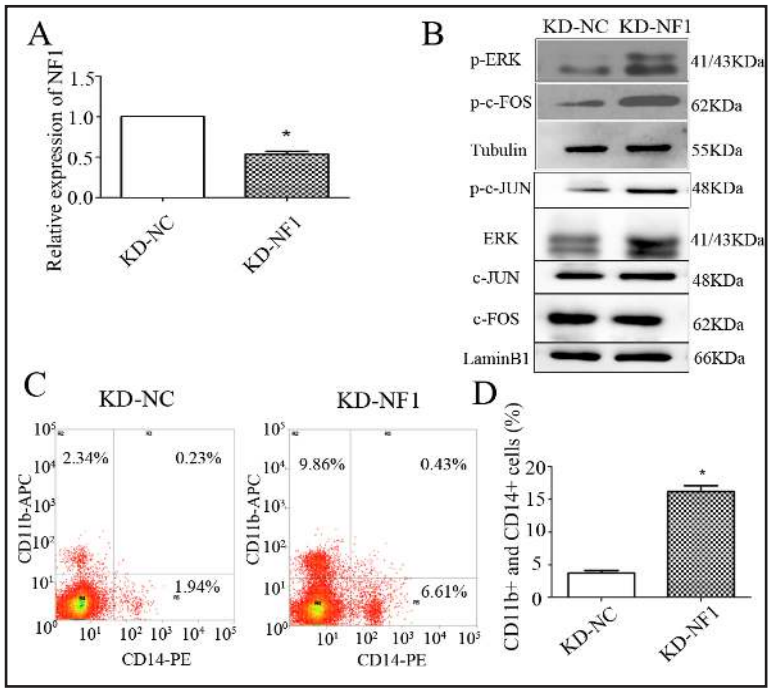

Fig. 7. NF1 loss promotes THP-1 cell differentiation by activating ERK signalling. (A) NF1 knockdown efficiency in THP-1 cells was determined by RT-qPCR. (B) NF1 knockdown up-regulated ERK, c-JUN and c-FOS phosphorylation (C) and increased CD11b and CD14 expression levels. (D) Percentages of $CD11b^+$ and $CD14^+$ cells in (C) are expressed as the mean ± SD of three independent experiments. *p<0.05.

Recent evidence has shown that differential miR expression levels are correlated with cellular responses to agents. MicroRNAs usually bind to the 3´-UTRs of target mRNAs; this binding results in translational suppression or mRNA degradation of numerous target genes [4]. According to many studies, chemicals can induce various effects in various cell types and regulate the expression of miRs. For instance, metformin can reduce miR-222 expression in the human lung cancer cell line A549 to inhibit cancer cell growth and cell cycle progression [23]. Additionally, Liu et al. reported that miR-143 expression was down-regulated in shikonin-treated glioblastoma stem cells (GSCs) and that miR-143 targets BAG3 to promote GSC apoptosis [24]. In our analysis, we found that miR-125a-3p expression was induced following LukS-PV treatment in THP-1 cells. Moreover, the results obtained from gain-of-function and loss-of-function approaches indicated that miR-125a-3p is involved in regulating differentiation and apoptosis in THP-1 cells *in vitro*. Lentiviral-mediated miR-125a-3p over-expression increased the expression levels of standard differentiation and apoptosis markers in THP-1 cells. These results confirm that miR-125a-3p acts as a cellular biological function regulator in THP-1 cells. MiR-125a-3p expression was down-regulated by the miR-silencing construct. This effect decreased the ability of LukS-PV to induce differentiation and apoptosis in THP-1 cells. These data confirm that miR-125a-3p plays a key role in the effects of LukS-PV on THP-1 cells.

To gain insight into the underlying molecular mechanisms through which miR-125a-3p influences differentiation and apoptosis in THP-1 cells, we used bioinformatics to predict its possible target genes. As shown in the database, NF1 and Bcl-2 were found to be targets of miR-125a-3p. Luciferase activity assays further confirmed that miR-125a-3p could directly target NF1 and Bcl-2. NF1 encodes a GAP that terminates Ras/mitogen-activated protein

kinase (MAPK) signalling by stimulating Ras•GTP hydrolysis to inactive Ras•GDP. NF1 inactivation leads to the hyperactivation of Ras and its downstream signalling components, such as the Raf/MAPK/ERK cascade [25-27]. Functional studies have indicated that NF1 participates in signalling pathways that are responsible for a variety of cellular processes. Nevertheless, the link between NF1 and differentiation in THP-1 cells has not been reported. Our results also indicated that LukS-PV can activate the ERK pathway to promote THP-1 cell differentiation [2]. For these reasons, we speculated that LukS-PV-regulated miR-125a-3p expression targets NF1 to promote THP-1 cell differentiation by activating the ERK pathway. In support of this hypothesis, we knocked down NF1 and found that ERK signalling and differentiation marker expression were promoted in THP-1 cells. However, many studies have shown that NF1 acts as a differentiation promoter to regulate leukaemia cells [28, 29], and these results are not consistent with ours. This discrepancy suggests that NF1 has various regulatory effects in different cellular contexts.

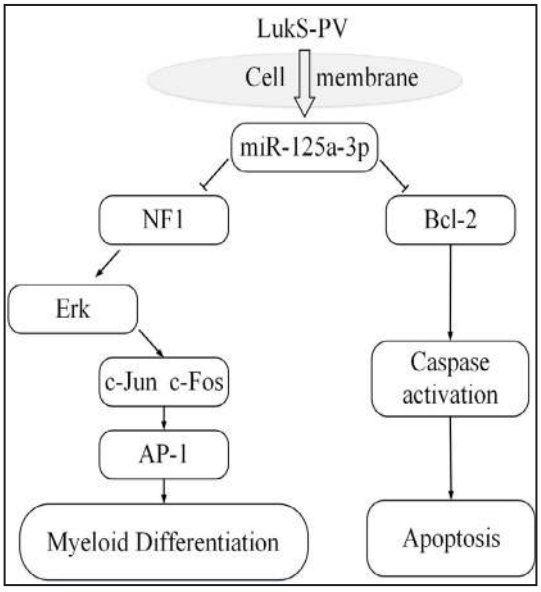

Fig. 8. Potential mechanisms of LukS-PV-regulated miR-125a-3p in THP-1 cells. In THP-1 cells, LukS-PV up-regulates the expression of miR-125a-3p. This up-regulation contributes to NF1 and Bcl-2 mRNA degradation, which causes JUN and FOS phosphorylation and the subsequent activation of the apoptosis cascade. The increase in AP-1 and caspase activation may regulate THP-1 cell differentiation and apoptosis.

Bcl-2 is a key negative regulator of apoptosis that controls intracellular Ca^{2+} release, oxygen free radical metabolism, and signal transduction pathways [30, 31]. Previous studies have reported that Bcl-2 regulates apoptosis by forming homodimers with Bax to prevent its release; thus, there is a relationship between Bcl-2 deficiency and increased Bax signalling [32]. In addition, Bcl-2 can inhibit cytochrome C release into the cytosol; this action activates caspase-3, caspase-8 and caspase-9 and leads to apoptosis [33]. Together, our results indicate that miR-125a-3p suppresses Bcl-2 expression to allow downstream caspase signalling activation to promote apoptosis in THP-1 cells.

The cellular response to any agent undoubtedly differs by cell type and treatment duration, and one agent may induce various effects by activating different regulatory mechanisms. In our study, we found that LukS-PV-regulated miR-125a-3p promotes THP-1 cell differentiation by targeting the NF1/ERK pathway while also promoting apoptosis by targeting the Bcl-2/caspase pathway (Fig. 8). Taken together, our results suggest that LukS-PV stimulates miR-125a-3p expression, which plays a critical role in THP-1 monocytes.

Acknowledgements

This study was supported by the National Natural Science Foundation (81572065) and the Anhui Provincial Natural Science Foundation (1408085MH188).

Disclosure Statement

There are no conflicts of interest for any author.

References

1 Genestier AL, Michallet MC, Prevost G, Bellot G, Chalabreysse L, Peyrol S, Thivolet F, Etienne J, Lina G, Vallette FM, Vandenesch F, Genestier L: Staphylococcus aureus Panton-Valentine leukocidin directly targets mitochondria and induces Bax-independent apoptosis of human neutrophils. J Clin Invest 2005;115:3117-3127.
2 Dai C, Zhang C, Sun X, Pan Q, Peng J, Shen J, Ma X: LukS-PV induces differentiation by activating the ERK signaling pathway and c-JUN/c-FOS in human acute myeloid leukemia cells. Int J Biochem Cell Biol 2016;76:107-114.
3 Bu S, Xie Q, Chang W, Huo X, Chen F, Ma X: LukS-PV induces mitochondrial-mediated apoptosis and G0/G1 cell cycle arrest in human acute myeloid leukemia THP-1 cells. Int J Biochem Cell Biol 2013;45:1531-1537.
4 Bartel DP: MicroRNAs: genomics, biogenesis, mechanism, and function. Cell 2004;116:281-297.
5 Calin GA, Croce CM: MicroRNA signatures in human cancers. Nat Rev Cancer 2006;6:857-866.
6 Kent OA, Mendell JT: A small piece in the cancer puzzle: microRNAs as tumor suppressors and oncogenes. Oncogene 2006;25:6188-6196.
7 Tian P, Yan L: Inhibition of MicroRNA-149-5p Induces Apoptosis of Acute Myeloid Leukemia Cell Line THP-1 by Targeting Fas Ligand (FASLG). Med Sci Monit 2016;22:5116-5123.
8 Lin HS, Gong JN, Su R, Chen MT, Song L, Shen C, Wang F, Ma YN, Zhao HL, Yu J, Li WW, Huang LX, Xu XH, Zhang JW: miR-199a-5p inhibits monocyte/macrophage differentiation by targeting the activin A type 1B receptor gene and finally reducing C/EBPalpha expression. J Leukoc Biol 2014;96:1023-1035.
9 Jiang L, Chang J, Zhang Q, Sun L, Qiu X: MicroRNA hsa-miR-125a-3p activates p53 and induces apoptosis in lung cancer cells. Cancer Invest 2013;31:538-544.
10 Yin F, Zhang JN, Wang SW, Zhou CH, Zhao MM, Fan WH, Fan M, Liu S: MiR-125a-3p regulates glioma apoptosis and invasion by regulating Nrg1 PLoS One 2015;10:e0116759.
11 Ufkin ML, Peterson S, Yang X, Driscoll H, Duarte C, Sathyanarayana P: miR-125a regulates cell cycle, proliferation, and apoptosis by targeting the ErbB pathway in acute myeloid leukemia. Leuk Res 2014;38:402-410.
12 Tu XM, Gu YL, Ren GQ: miR-125a-3p targetedly regulates GIT1 expression to inhibit osteoblastic proliferation and differentiation. Exp Ther Med 2016;12:4099-4106.
13 Aldo PB, Craveiro V, Guller S, Mor G: Effect of culture conditions on the phenotype of THP-1 monocyte cell line. Am J Reprod Immunol 2013;70:80-86.
14 Qin Z: The use of THP-1 cells as a model for mimicking the function and regulation of monocytes and macrophages in the vasculature. Atherosclerosis 2012;221:2-11.
15 Yang S, Li F, Jia S, Zhang K, Jiang W, Shang Y, Chang K, Deng S, Chen M: Early secreted antigen ESAT-6 of Mycobacterium Tuberculosis promotes apoptosis of macrophages via targeting the microRNA155-SOCS1 interaction. Cell Physiol Biochem 2015;35:1276-1288.
16 Yang Y, Yang L, Liang X, Zhu G: MicroRNA-155 Promotes Atherosclerosis Inflammation via Targeting SOCS1 Cell Physiol Biochem 2015;36:1371-1381.
17 Yin Y, Li F, Shi J, Li S, Cai J, Jiang Y: MiR-146a Regulates Inflammatory Infiltration by Macrophages in Polymyositis/Dermatomyositis by Targeting TRAF6 and Affecting IL-17/ICAM-1 Pathway. Cell Physiol Biochem 2016;40:486-498.
18 Ma X, Chang W, Zhang C, Zhou X, Yu F: Staphylococcal Panton-Valentine leukocidin induces pro-inflammatory cytokine production and nuclear factor-kappa B activation in neutrophils. PLoS One 2012;7:e34970.
19 Colin DA, Mazurier I, Sire S, Finck-Barbancon V: Interaction of the two components of leukocidin from Staphylococcus aureus with human polymorphonuclear leukocyte membranes: sequential binding and subsequent activation. Infect Immun 1994;62:3184-3188.
20 Yoong P, Pier GB: Immune-activating properties of Panton-Valentine leukocidin improve the outcome in a model of methicillin-resistant Staphylococcus aureus pneumonia. Infect Immun 2012;80:2894-2904.
21 Graves SF, Kobayashi SD, Braughton KR, Whitney AR, Sturdevant DE, Rasmussen DL, Kirpotina LN, Quinn MT, DeLeo FR: Sublytic concentrations of Staphylococcus aureus Panton-Valentine leukocidin alter human PMN gene expression and enhance bactericidal capacity. J Leukoc Biol 2012;92:361-374.

22 Holzinger D, Gieldon L, Mysore V, Nippe N, Taxman DJ, Duncan JA, Broglie PM, Marketon K, Austermann J, Vogl T, Foell D, Niemann S, Peters G, Roth J, Loffler B: Staphylococcus aureus Panton-Valentine leukocidin induces an inflammatory response in human phagocytes via the NLRP3 inflammasome. J Leukoc Biol 2012;92:1069-1081.
23 Wang Y, Dai W, Chu X, Yang B, Zhao M, Sun Y: Metformin inhibits lung cancer cells proliferation through repressing microRNA-222 Biotechnol Lett 2013;35:2013-2019.
24 Liu J, Qu CB, Xue YX, Li Z, Wang P, Liu YH: MiR-143 enhances the antitumor activity of shikonin by targeting BAG3 expression in human glioblastoma stem cells. Biochem Biophys Res Commun 2015;468:105-112.
25 Martin GA, Viskochil D, Bollag G, McCabe PC, Crosier WJ, Haubruck H, Conroy L, Clark R, O'Connell P, Cawthon RM, et al.: The GAP-related domain of the neurofibromatosis type 1 gene product interacts with ras p21 Cell 1990;63:843-849.
26 Ballester R, Marchuk D, Boguski M, Saulino A, Letcher R, Wigler M, Collins F: The NF1 locus encodes a protein functionally related to mammalian GAP and yeast IRA proteins. Cell 1990;63:851-859.
27 Basu TN, Gutmann DH, Fletcher JA, Glover TW, Collins FS, Downward J: Aberrant regulation of ras proteins in malignant tumour cells from type 1 neurofibromatosis patients. Nature 1992;356:713-715.
28 Lauchle JO, Kim D, Le DT, Akagi K, Crone M, Krisman K, Warner K, Bonifas JM, Li Q, Coakley KM, Diaz-Flores E, Gorman M, Przybranowski S, Tran M, Kogan SC, Roose JP, Copeland NG, Jenkins NA, Parada L, Wolff L, Sebolt-Leopold J, Shannon K: Response and resistance to MEK inhibition in leukaemias initiated by hyperactive Ras. Nature 2009;461:411-414.
29 Park JI, Powers JF, Tischler AS, Strock CJ, Ball DW, Nelkin BD: GDNF-induced leukemia inhibitory factor can mediate differentiation via the MEK/ERK pathway in pheochromocytoma cells derived from nf1-heterozygous knockout mice. Exp Cell Res 2005;303:79-88.
30 Mathai JP, Germain M, Shore GC: BH3-only BIK regulates BAX,BAK-dependent release of Ca2+ from endoplasmic reticulum stores and mitochondrial apoptosis during stress-induced cell death. J Biol Chem 2005;280:23829-23836.
31 Brooks C, Dong Z: Regulation of mitochondrial morphological dynamics during apoptosis by Bcl-2 family proteins: a key in Bak? Cell Cycle 2007;6:3043-3047.
32 Cory S, Adams JM: The Bcl2 family: regulators of the cellular life-or-death switch. Nat Rev Cancer 2002;2:647-656.
33 Zhao L, Yan X, Shi J, Ren F, Liu L, Sun S, Shan B: Ethanol extract of Forsythia suspensa root induces apoptosis of esophageal carcinoma cells via the mitochondrial apoptotic pathway. Mol Med Rep 2015;11:871-880.